J Solid State Electrochem (2007) 11:869–876
DOI 10.1007/s10008-007-0276-6

REVIEW PAPER

Electroless deposition and some properties of Ni–Cu–P and Ni–Sn–P coatings

J. Georgieva · S. Armyanov

Received: 30 September 2006 / Revised: 8 January 2007 / Accepted: 10 January 2007 / Published online: 7 February 2007

Abstract In this review, a summary of our published results, completed with new unpublished data are considered together with some of other authors' publications, making an attempt to reveal the mechanism of the third element co-deposition in electroless Ni–P plating and to define its influence on the ternary coatings' properties. A model explaining the triple role of Cu added to the solution for electroless (EL) Ni–P plating is described: as a stabilizer [Cu(I)]; as an accelerator; and as a stability-affecting agent, forming a dispersed solid phase in the solution. The disproportionation reaction of Cu(I) has been taken into account. A planned experiment was performed using full-effect factorial design with two levels of three process variables, and the response surfaces were constructed. The interaction between the factors was revealed. The results are in harmony with the aforementioned model. In low-tin Ni–Sn–P coatings, the alloy components are uniformly distributed both on the surface and through the thickness. In contrast, high-tin coatings exhibit three-dimensional areas enriched in Sn and impoverished in Ni and P. As the reason for their formation, the disproportionation reaction of Sn(II) is suggested, supposed to be locally predominant over the hypophosphite oxidation. EL deposition of pure Sn onto Ni–Sn–P substrates is shown. The inclusion of Cu or Sn in EL Ni–P increases the thermal stability of amorphous state, ensures the preservation of a paramagnetic behavior and improves the corrosion resistance.

Keywords Electroless Ni–Cu–P · Electroless Ni–Sn–P · Ternary alloys · Thermal stability · Disproportionation

Introduction

Reviewing the growing achievements in theory and practice of electroless (autocatalytic) plating, the contribution of the Institute of Chemistry (Institute of Chemistry and Chemical Technology 1945–1992) of the Lithuanian Academy of Sciences cannot be omitted [1–3].

During the last 10–15 years, the attention to the electroless plating of nickel-based ternary alloys has been increased because of their excellent corrosion, wear, and thermal stability and electrical resistance. Their industrial application is expanding too. In more detail, since 1990, about 70 papers and patents on electroless plating of ternary Ni–Cu–P coatings appeared. The reason for such an interest is that inclusion of Cu in electroless Ni–P alloys improves their smoothness [4, 5], brightness [5, 6], and corrosion resistance [7, 8]. The application of Ni–Cu–P in VLSI [9–11] and thin-film memory disks [12, 13] has been considered.

Low-tin coatings possess a high corrosion resistance [14–17]. Alkaline solutions have been used for the deposition of Ni–Sn–P coatings of higher tin content, and the application of stannous [Sn(II)] ions as a tin source seems more prospective than stannic [Sn(IV)] ions. When the tin content is up to 10.4 at.%, an amorphous structure was noticed at a lower content of phosphorus than what happens in Ni–P alloys [18, 19]. At higher tin contents (14 at.%), the crystalline structure appears, and the crystallinity of Ni–Sn–P alloys increases with a further increase in tin content [20]. The best anticorrosion behavior is displayed by a Ni–Sn–P coating with either low crystallinity or amorphous structure and high tin content

Dedicated to the 70th birthday of Professor A. Vaskelis.

J. Georgieva · S. Armyanov (✉)
Rostislaw Kaischew Institute of Physical Chemistry,
Bulgarian Academy of Science,
Acad.G.Bonchev str., Bld. 11,
1113 Sofia, Bulgaria
e-mail: armyanov@venera.ipc.bas.bg

[20, 21]. The solderability of Ni–Sn–P exceeds that of Ni–P, and it is improved with increasing tin content [20, 22].

The addition of limited quantities of Cu [23–25] and Sn [17, 24, 26] in Ni–P alloys improves their thermal stability, which means preservation of their amorphous state and paramagnetic behavior.

In the same time, the mechanism of co-deposition of a third element, and particularly, tin and copper during the electroless plating of Ni–P is still not clear enough. Initially the use of monovalent cuprous [Cu(I)] ions in the electroless Ni–P baths averted the problem of sulfur co-deposition observed with sulfur containing stabilizers [27]. With Cu(I) ions, the solution stability was improved without significantly retarding the plating rate. Later, it was revealed that even the cupric [Cu(II)] ions had a similar stabilizing effect [5, 28–30]. An increase in the deposition rate and a decrease in phosphorus content of the electroless nickel was noticed when Cu(II) ions were added to the plating solution [5, 29–32]. A rise in hypophosphite utilization efficiency was also mentioned [5, 29, 30]. A critical survey of the literature suggests that there is much ambiguity with regard to the proposed mechanisms for the role of copper in the process of electroless Ni–P plating. For example, copper is known to stabilize the solution, but simultaneously, it increases the deposition rate. In summary, the nature of favorable effects of copper on the solution stability and on the efficiency of hypophosphite utilization in Ni–P electroless plating is under investigation [6, 33].

The co-deposition of tin is a challenging problem also. It should be reminded that Sn(II) ions were initially used as a stabilizer of electroless Ni–P plating [34–37]. In this way, their presence in the bath in high amount suppresses the electroless plating and can even stop it. The uniformity of Ni–Sn–P coatings was not a subject of special interest, and the data about the tin distribution through the coating thickness is very scarce [38]. On the other hand, it was proved that the electroless tin plating in strong alkaline solutions might be accomplished by the disproportionation reaction [39, 40]. This process was further developed [41, 42] and the role of tin catalytic surface was indicated [43]. However, the role of disproportionation reaction in the electroless deposition of tin-rich Ni–Sn–P coatings is very interesting also [44]. The disproportionation reaction may have a role during the electroless plating of Ni–Cu–P, too [33].

The aim of this review is to summarize our experience in investigating the process of co-deposition of copper and tin during electroless plating of Ni–Cu–P [33, 45] and Ni–Sn–P [44] coatings taking into account the role of disproportionation reactions of Cu(I) and Sn(II), respectively. Our unpublished data on the properties of Ni–Cu–P and Ni–Sn–P, including the corrosion behavior of electroless Ni–Cu–P and Ni–Sn–P alloys, deposited on Al from acidic solutions, will be presented. A discussion of some of the other authors' publications will be given, trying to reveal the mechanism of the third element co-deposition in electroless Ni–P plating and to outline its influence on the ternary coatings' properties. The homogeneity and elemental distribution in the tin-enriched Ni–Sn–P coatings plated electrolessly in alkaline solutions will be considered.

Materials and methods

The solutions for Ni–Cu–P electroless deposition were based on a citric–acetic acidic bath containing sodium hypophosphite as a reducing agent [46, 47]. The concentration of sodium acetate and sodium citrate was increased from the recommended concentration for electroless Ni–P plating [47] to the final levels of 0.20 and 0.16 M, respectively. Glycine was also included in the plating solution: 0.28 M. Additional modifications of the bath composition were necessary to prevent a decrease in phosphorus content in the alloy due to copper co-deposition. The concentrations of nickel and hypophosphite in the working bath were 0.10 and 0.36 M, respectively. The deposition was carried out at a temperature of 88±1 °C and pH of 4.7. Due to the presence of copper in the solution, no other stabilizers were used. Continuous replenishment was applied to keep constant the solution concentration and especially copper at the level of 15± 2 ppm determined by atomic absorption spectroscopy (AAS) analysis. While investigating the role of bath components in a planned experiment, additional modifications of the composition were made as it is shown further in the text. Supplementary details about the deposition of Ni–Cu–P and experiments of conducted investigations can be found in Armyanov et al. and Georgieva and Armyanov [33, 45].

The deposition of Ni–Sn–P was performed in a bath based on an alkaline citrate ammonia-free solution for electroless plating of Co–Ni–P alloy [46, 48]. The solution buffering was carefully made along with a proper choice of complexing agents (citrate, boric acid, and aminoalcohols) to ensure pH stability in the alkaline region and to prevent precipitation of metal hydroxides [46]. The typical solution for Ni–Sn–P coatings contained $NiSO_4 \cdot 6H_2O$ 0.05 M, hypophosphite 0.20 M, citrate 0.20 M, and H_3BO_3 0.02 M. The electroless plating was conducted at 90 °C and pH 9–10. Sn(II) concentration in this solution was varied from 0.4 to 1.5 mM and no other stabilizers were used. More information about the experimental conditions can be found in Georgieva et al. [44].

Electrochemical corrosion tests were conducted in 5% sodium chloride and 0.5 M sulfuric acid solutions to compare the corrosion behavior of electroless Ni–Cu–P and Ni–Sn–P alloys with Ni–P. The ternary coatings and

the Ni–P were deposited from acidic electrolytes of similar compositions with the addition of Cu(II) and Sn(IV) ions, respectively. To improve the adhesion of the Ni–Sn–P coatings, a thin Ni–Cu–P under layer (strike) was electrolessly deposited on Al substrate. Samples were selected targeting comparable phosphorus content (about 11 wt%) with the coating thickness 15–20 μm. The experiments were performed using Autolab 30 (EcoChemie) in a three-electrode cell. A saturated calomel electrode (SCE) was applied as the reference electrode and a Pt foil as the counter electrode. The samples were first immersed into the electrolyte for about 20 min to stabilize the open-circuit potential (OCP). Potentiodynamic polarization studies (Tafel plots) were carried out by polarizing the working electrode from the OCP to 250 mV in cathodic direction and 400 mV in anodic direction at a scan rate 1 mV/s. The corrosion current densities (i_{corr}) were determined by extrapolating the straight-line section of the anodic and cathodic branches of the Tafel curves in the vicinity of the corrosion potential (±25 mV) using the software installed in the instrument.

Results and discussion

A simple model has been proposed, which explains the role of copper added to the acidic solution for electroless nickel plating (Fig. 1) [33]. This model assumes that the adsorbed Cu(II) ions are reduced equally into the Cu (co-deposited in the alloy) and Cu(I) ions (adsorbed on the surface) by reactions with hypophosphite as follows:

$$\mathrm{Cu(II)} + 2\mathrm{H_2PO_2^-} + 2\mathrm{H_2O} \xrightarrow{\mathrm{Ni}} \mathrm{Cu} + 2\mathrm{H_2PO_3^-} + \mathrm{H_2} + 2\mathrm{H^+} \quad (1)$$

$$2\mathrm{Cu(II)} + 2\mathrm{H_2PO_2^-} + 2\mathrm{H_2O} \xrightarrow{\mathrm{Ni}} 2\mathrm{Cu(I)} + 2\mathrm{H_2PO_3^-} + \mathrm{H_2} + 2\mathrm{H^+} \quad (2)$$

These two autocatalytic reactions with hypophosphite occur only in the presence of Ni because Cu does not catalyze hypophosphite oxidation [49–52]. The partially reduced (according to Eq. 2) to Cu(I) ions are equally distributed: half of them possibly act as a stabilizer, while the others take part in the disproportionation reaction (Eq. 3), generating fine Cu powder dispersed randomly throughout the solution):

$$2\mathrm{Cu(I)} \rightarrow \mathrm{Cu} + \mathrm{Cu(II)} \quad (3)$$

In accordance with the model (Fig. 1 and Eqs. 1–3), the precipitated copper powder accounts for a quarter of the initial concentration of copper. This cycle (reactions 1–3) repeats many times, and a geometric progression formula can be used to calculate the total amount of precipitated copper [33]. Thus, the described model predicts that approximately two-thirds of the consumed copper will be co-deposited in the alloy. The remaining one-third is lost as copper powder formed due to the disproportionation reaction (Eq. 3). Measures should be taken to ensure the removal of precipitated copper from the bath, especially when its usage is long-term and continuous filtration is not applied. In a similar manner, this disproportionation reaction is recognized as a cause for the instability of the electroless copper plating solutions. This reaction explains the observation of solid copper precipitates, when the copper concentration in the Ni–Cu–P plating bath is increased.

From the other side, being nobler than Ni, copper could be preferentially deposited forming Cu-rich zone near the substrate [6, 53–55]. Its formation is due to the predominant deposition of Cu, unless it is not bound in a strong enough complex, which shifts negatively its potential bringing it near that of the Ni(II) ion, which is also complexed. Only after fulfillment of this condition can the parallel deposition of Ni and Cu occur. This necessitates a delicate balance of the concentrations of Cu and a specific type of complexing agent or a combination of complexing agents. Thus, an additional complication arises in the composition and maintaining of the solution for electroless Ni–Cu–P plating.

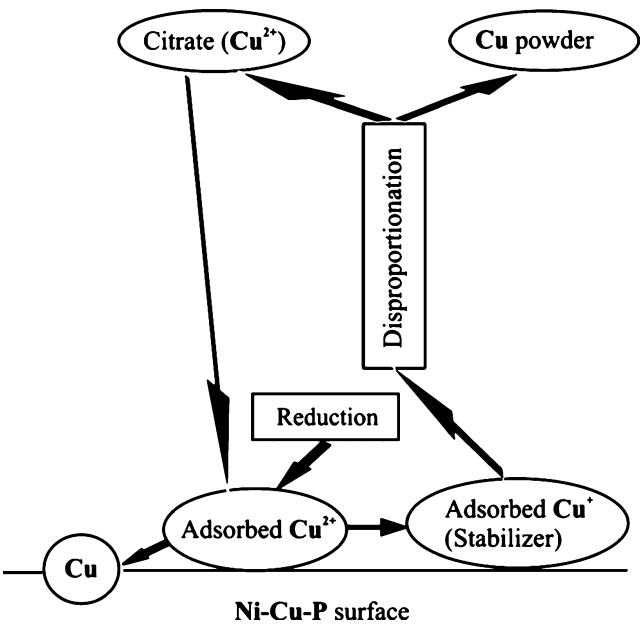

Fig. 1 Schematic presentation of the copper co-deposition during electroless Ni–Cu–P plating

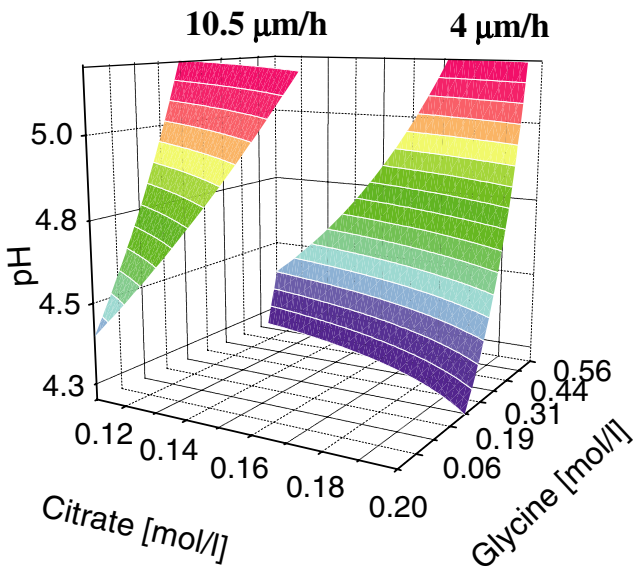

Fig. 2 Response surfaces for the deposition rates (V) 4 and 10 µm/h as a function of citrate and glycine concentration and pH of the bath [45]

The observed enhancement of the deposition rate should be attributed to the improved catalytic activity of the electroless Ni–Cu alloy [56]. The increased catalytic activity was suggested to be primarily due to the weaker chemisorption of hydrogen on the Ni–Cu surface, in comparison with pure nickel.

The experimental verification of the described above model (Fig. 1 and Eqs. 1–3) during the prolonged operation of the solution (more than two Ni turnover) shows very good correspondence between the expected by the model and the determined amount of copper in the coating [33]. The latter was assessed precisely by AAS analyses of samples of the ternary alloys. In this way, the model

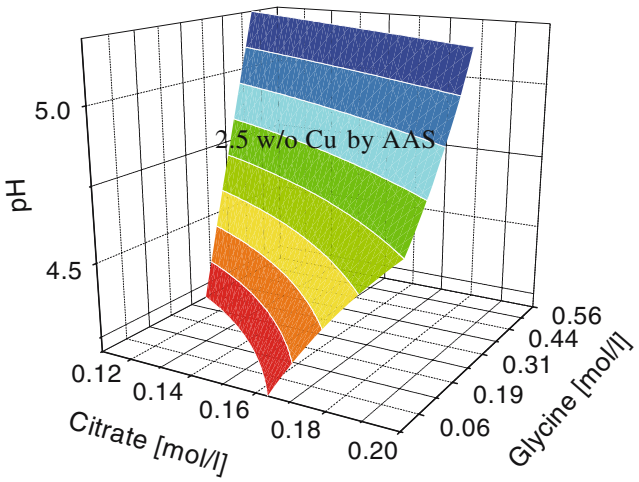

Fig. 3 The response surface for the copper content of 2.5 wt% in the coating as a function of citrate and glycine concentration and pH of the bath [45]

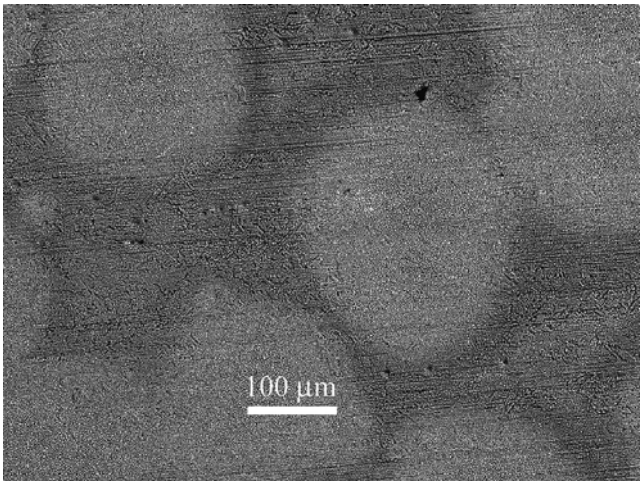

Fig. 4 SEM (back-scattered electron) image of electroless high-tin Sn–Ni–P coating [44]

explains the relationship between three different roles of Cu added to the solution for electroless nickel plating, which have been observed by other authors also: as a stabilizer [Cu(I)]; as an accelerator (due to the catalytic properties of Ni–Cu alloys); and as a stability-affecting agent (due to the formation of randomly dispersed copper particles in the solution) [33].

Further contribution to investigations of electroless Ni, Cu, and P co-deposition was made by performing a planned experiment. The full-effect factorial design (FD) was applied with three factors at two levels of the process variables: bath pH (x_1) and concentrations of two complexing agents: citrate (x_2) and glycine (x_3) on the rate of deposition (V) and content of Cu and P in the deposit [45]. This FD experiment allows observation of the effects of each factor at different levels of the other variables and the interactions between these factors. The aim was to use the statistical techniques to build reliable models for the electro-

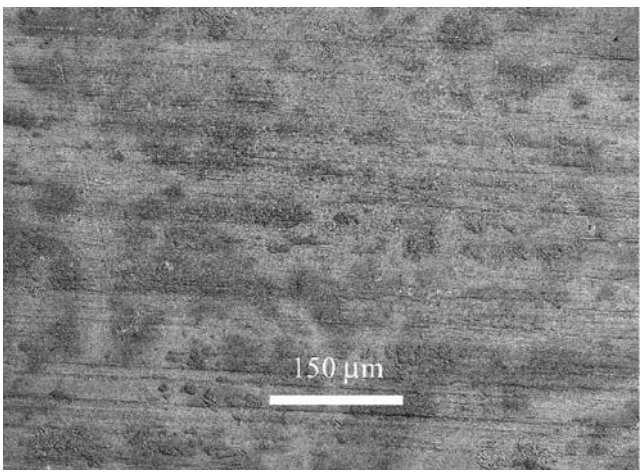

Fig. 5 SEM (back-scattered electron) image of electroless deposited Sn–Ni–Cu–P coating [44]

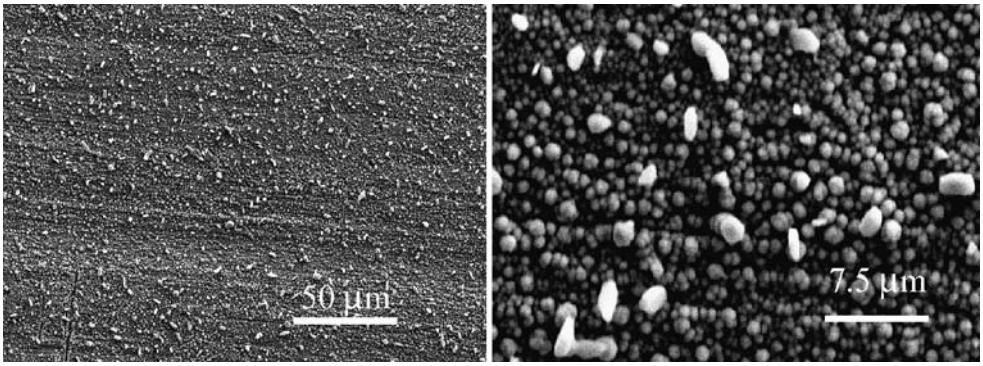

Fig. 6 SEM image of electroless deposited pure Sn onto low-tin Ni–Sn–P alloy. Two magnifications are shown

less deposition of Ni–Cu–P and to construct the response surfaces. The obtained regression models were:

$$V = 6.61 + 2.84x_1 - 2.91x_2 - 1.66x_3 - 1.39x_1x_2 + 0.76x_2x_3 - 0.54x_1x_3 \quad (4)$$

$$\mathrm{Cu} = 2.60 - 0.48x_1 + 0.52x_2 + 0.32x_3 + 0.15x_1x_2 - 0.10x_2x_3 - 0.10x_1x_3 + 0.18x_1x_2x_3 \quad (5)$$

$$P = 12.19 - 0.19x_1 + 0.41x_2 + 0.26x_3 + 0.59x_1x_2 \quad (6)$$

All obtained regression models include interactions between the variables. The deposition rate (V) and copper content in the alloy are affected the most powerfully by pH and citrate concentration (Figs. 2, 3). Phosphorus content depends mainly on the citrate concentration and interaction between solution acidity and citrate concentration in the bath. Within the range of factors variations, in the current FD experiment pH does not affect strongly P content in the alloy, which is useful for some applications. All three controlled parameters (deposition rate, Cu, and P content in the alloy) have been affected by both glycine and citrate concentration, although the effect of glycine is weaker. The model and the response surfaces (Figs. 2, 3) have been used to design Ni–Cu–P coatings with various copper concentrations.

The electroless deposition of Ni–Sn–P coatings shows more particularities depending on bath and deposit compositions. In low-tin Ni–Sn–P coatings, there is a uniform distribution of the alloy components, both on the surface and through the thickness [44]. The main mechanism of electroless alloy deposition, in this case, is based on the well-known hypophosphite oxidation as a source of electrons for the metals (Sn and Ni) and P reduction.

In high-tin Sn–Ni–P coatings, there is a nonuniform distribution of the components. Using Auger electron spectroscopy (AES), scanning AES, and scanning electron microscopy with energy-dispersive X-ray spectroscopy, three-dimensional areas enriched in tin and impoverished in Ni and P have been observed and investigated [44]. Their view from the surface is shown in Fig. 4. Bright areas are

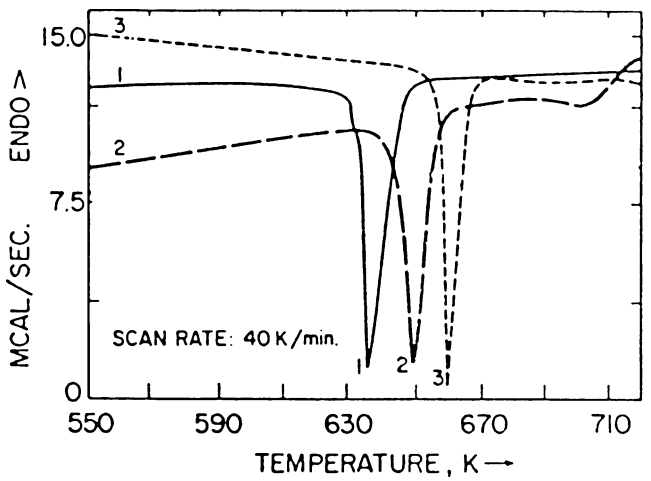

Fig. 7 Differential scanning calorimetry curves of devitrification of: *1* Ni-11.9P; *2* Ni-1.7Cu-12.2P; *3* Ni-1.1Sn-11.0P (The content of P, CU and Sn is in wt%)

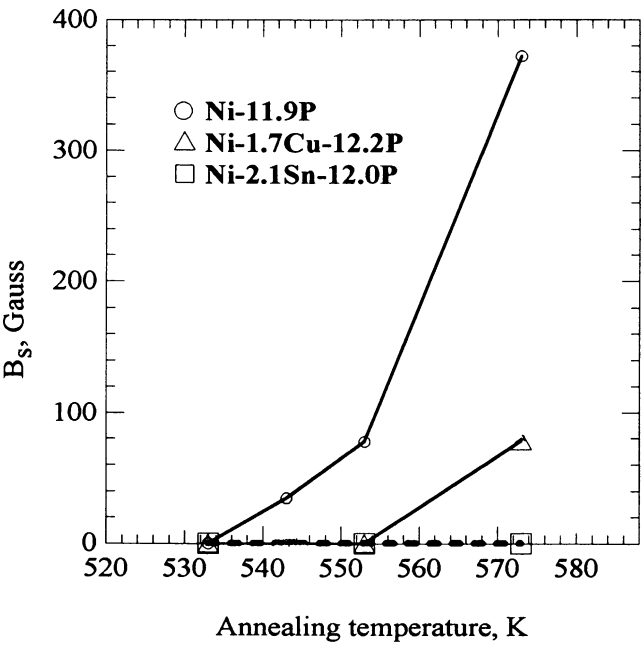

Fig. 8 Saturation induction, B_s vs annealing temperature of heat treated during 1 h Ni–P, Ni–Sn–P, and Ni–Cu–P deposits (The content of P, Cu and Sn is in wt%)

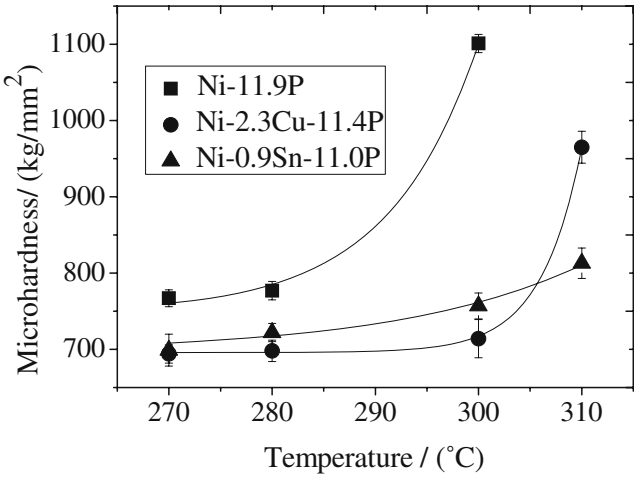

Fig. 9 Microhardness vs annealing temperature for Ni–P and Ni–Me–P coatings (The content of P, Cu, and Sn is in wt%)

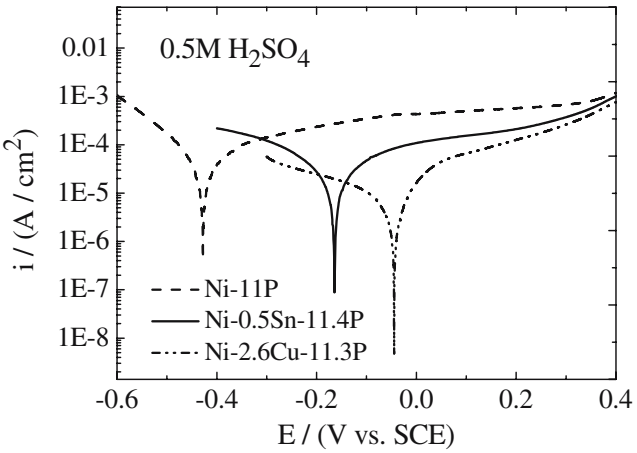

Fig. 11 Potentiodynamic polarization curves of electroless Ni–Cu–P, Ni–Sn–P, and Ni–P alloys in 0.5 M sulfuric acid solution (The content of P, Cu, and Sn is in wt%)

enriched in tin. The disproportionation reaction of Sn(II) (see Eq. 7 below) is suggested as being predominant over the hypophosphite oxidation in these three-dimensional areas and is responsible for their formation. Thus, the creation of high-tin Sn–Ni–P coatings is probably the result of two electroless processes which are not taking place uniformly at the different areas of the deposit [44]:

1) A reduction of Ni, Sn, and P due to the hypophosphite oxidation, similar to the process illustrated by Eq. 1.
2) The tin disproportionation (in alkaline conditions):

$$2HSnO_2^- + 2H_2O \xrightarrow{Sn} Sn + Sn(OH)_6^{2-} \quad (7)$$

The distribution of Sn in high-tin Sn–Ni–Cu–P coatings is not uniform also, similar to high-tin Sn–Ni–P (Fig. 5). However, the introduction of copper in the solution gives an additional opportunity to reveal the role of the oxidation of Sn (II) into Sn(IV) as a source of electrons. It is observed that the areas enriched in Sn contain increased Cu content [44]. Thus, to the aforementioned two processes, a new one is added:

3) The copper reduction due to the Sn(II) oxidation:

$$Cu(II) + HSnO_2^- + H_2O + 3OH^- \rightarrow Cu + Sn(OH)_6^{2-} \quad (8)$$

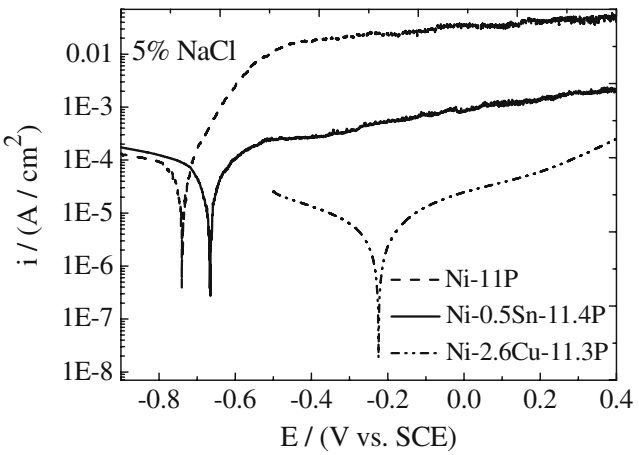

Fig. 10 Potentiodynamic polarization curves of electroless Ni–Cu–P, Ni–Sn–P, and Ni–P alloys in 5% sodium chloride solution (The content of P, Cu, and Sn is in wt%)

Electroless deposition of pure Sn was made onto two kinds of substrates: low-tin and high-tin Ni–Sn–P alloys. This is possible through the disproportionation reaction, Eq. 7, due to the catalytic effect of these substrates for tin reduction, as it was mentioned in the introduction. The electroless tin coating is not continuous on any of these substrates, and it consists of separate grains. However, the obtained Sn crystals are almost identical in size and uniformly distributed when low-tin Ni–Sn–P serves as a substrate (Fig. 6). On the other part, the feasibility of electroless deposition of tin based on the disproportionation reaction on these substrates proves that this phenomenon is taking place also during the formation of tin-rich zone in the electroless plating of Sn–Ni–P coatings, as it is described above.

Table 1 Corrosion characteristics of electroless Ni–Cu–P, Ni–Sn–P, and Ni–P alloys in 5% sodium chloride and 0.5 M sulfuric acid solutions

Alloy	5% NaCl		0.5 M H_2SO_4	
	E_{corr} (mV vs SCE)	i_{corr} (μA/cm^2)	E_{corr} (mV vs SCE)	i_{corr} (μA/cm^2)
Ni-2.6Cu-11.3P	−223	0.7	−43	1.5
Ni-0.5Sn-11.4P	−679	6.4	−164	5.3
Ni-11P	−740	24.3	−429	13.5

The content of P, Cu, and Sn is in wt%.

It was established that the addition of Sn (1–2 wt%) or Cu (3–4 wt%) to high phosphorus (>10 wt% P) coatings increases the crystallization temperature of the amorphous Ni–P, as shown in Fig. 7 [24]. On the other side, according to the basic principles of ferromagnetism, the inclusion of elements, such as Cu and Sn in the Ni–P alloys, can decrease the magnetization of the precipitated ferromagnetic nickel phase during crystallization. Ni–Sn–P deposits remain nonmagnetic even after annealing at 573 K, while Ni–P and Ni–Cu–P become ferromagnetic after annealing at 543 or 553 K, respectively (Fig. 8). Therefore, complementary to the raised crystallization temperature, the third element affects the magnetic properties of the precipitating Ni-based phase due to alloying. The addition of Sn or Cu to the Ni–P leads to the incorporation of the third element into the precipitated Ni nanoparticles [57]. As both Sn and Cu decrease the spontaneous magnetization of Ni, they diminish the overall magnetization of the Ni–Sn–P and Ni–Cu–P alloy.

The effect of Cu and Sn on the microhardness of the deposits after annealing is shown in Fig. 9. The obtained results are in harmony with the data concerning the thermal stability of Ni–Cu–P and Ni–Sn–P alloys: the increase of microhardness with the temperature is retarded due to the delay of the devitrification processes caused by the third element.

The obtained potentiodynamic polarization curves of Ni–Cu–P, Ni–Sn–P, and Ni–P alloys in 5% NaCl and 0.5 M H_2SO_4 are presented in Figs. 10 and 11. The corrosion characteristics (E_{corr} and i_{corr}) of electroless Ni–Cu–P, Ni–Sn–P, and Ni–P alloys obtained from the Tafel polarization curves are listed in Table 1. The results show that the co-deposition of the third element causes a positive sift (with respect to Ni–P) of the corrosion potential of Ni–Cu–P and Ni–Sn–P in both NaCl and H_2SO_4. The corrosion current density values of Ni–Cu–P and Ni–Sn–P alloys are lower than those of Ni–P. The data in the literature about the corrosion behavior of amorphous Ni–Sn–P ternary alloys are scarce and occasionally conflicting. However, our results indicate that the Sn addition to alloys with high phosphorus content results in an improvement of their corrosion resistance, which is in agreement with data reported by other authors [58].

Conclusions

The role of disproportionation of Cu(I) and Sn(II) during the electroless plating of, respectively, Ni–Cu–P and high tin Sn–Ni–P coating is explained. The conditions for deposition of homogeneous Ni–Cu–P and Ni–Sn–P alloys are outlined. It is illustrated that complementary to the raised crystallization temperature, the addition of Sn or Cu to Ni–P decreases the magnetization of the precipitating Ni-based phase due to alloying. In this way, the thermal stability of the amorphous and paramagnetic state of the ternary Ni–Cu–P and Ni–Sn–P alloys is increased. The introduction of Cu or Sn as a third component improves considerably the corrosion resistance of Ni–P alloys. Electroless deposition of tin onto Ni–Sn–P coatings is demonstrated.

References

1. Šalkauskas M, Vaškelis A, (1985) Chemical metallizing of plastics, 3-d revised edition). Khimiya, Leningrad (in Russian)
2. Vaškelis A, Šalkauskas M (1986) Electroless plating. In: Satas D (ed) Plastics finishing and decoration. Van Nostrand Reinhold, New York, p 287
3. Vaškelis A (1991) Electroless plating. In: Satas D (ed) Coatings technology handbook. Dekker, New York, p 187
4. Balaraju JN, Rajam KS (2005) Surf Coat Technol 195:154
5. Tarozaitë R, Selskis A (2006) Trans Inst Met Finish 84(2):105
6. Chen C-H, Chen B-H, Hong L (2006) Chem Mat 18:2959
7. Zhao Q, Liu Y, Abel EW (2004) Mater Chem Phys 87:332
8. Liu Y, Zhao Q (2004) Appl Surf Sci 228:57
9. Dubin VM (1992) J Electrochem Soc 139:633
10. Chen C-J, Lin K-L (2000) J Electron Mater 29:1007
11. Chen C-J, Lin K-L (2001) IEEE Trans Compon Packag Technol 24:691
12. Zhong LL, Liu CC (2000) US Pat 6 106 927
13. Zhong LL, Liu CC, John St, Jeff D (2002) US Pat 6 410 104
14. Cavallotti P-L, Salvago G (1968) Electrochim Met 3:23
15. Aoki K, Takano O, Ishibashi S, Hayashi T (1978) Kinzoku Hyomen Gijutsu (J Metal Finish Soc Japan) 29:16
16. Mallory GO, Horn TR (1979) Plat Surf Finish 66(4):40
17. Mallory GO (1974) Trans Inst Met Finish 52:156
18. Bangwei Z, Haowen X (2000) Mater Sci Eng A 281:286
19. Haowen X, Bangwei Z, Qiaoqin Y (1999) Trans Inst Met Finish 77(3):99
20. Shimauchi H, Ozawa S, Tamura K, Osaka T (1994) J Electrochem Soc 141:1471
21. Aoki K, Takano O (1980) Kinzoku Hyomen Gijuisu (J Met Finish Soc Japan) 31:555
22. Aoki K, Takano O (1981) Kinzoku Hyomen Gijuisu (J Met Finish Soc Japan) 32:643
23. Krasteva N, Fotti V, Armyanov S (1994) J Electrochem Soc 141:2864
24. Krasteva N, Armyanov S, Georgieva J, Avramova N, Fotti V (1995) J Electron Mater 24:941
25. Yu H-S, Luo S-F, Wang Y-R (2001) Surf Coat Technol 148:143
26. Balaraju J N, Jahan S M, Jain A, Rajam K S (2006) J Alloys Compd, DOI 10.1016/j.jallcom.2006.07.045
27. Gulla M (1973) US Pat 3764 352
28. Tarozaitë R, Luneckas A (1981) Liet TSR Mokslu Akad Darbai, Serija B 5(126):19
29. Tarozaitë R, Luneckas A (1986) Liet TSR Mokslu Akad Darbai, Serija B 4(155):3
30. Tarozaitë R (2005) Chemija (Vilnius) 16(1):8
31. Bielinski J, Goldon A, Socko B, Bielinska A (1983) Metalloberflaeche 37:300
32. Bielinski J, Skudlarska E (1985) Oberfläche-Surf 26(3):76
33. Armyanov S, Georgieva J, Tachev D, Valova E, Nyagolova N, Mehta S, Leibman D, Ruffini A (1999) Electrochem Solid State Letters 2:323

34. Gutzeit G, Ramirez EJ (1953) US Pat 2 658 841
35. Talmey P, Gutzeit G (1956) US Pat 2 762 723
36. Gurzeit G (1960) Plating 47:63
37. Bielinski J, Bielinska A, Gluszewski W (1983) Metalloberfläche 37(3):112
38. Armyanov S, Steenhaut O, Krasteva N, Georgieva J, Delplancke J-L, Winand R, Vereecken J (1996) J Electrochem Soc 143:3692
39. Pil'nikov VP, Osyagina VA (1979) Zhurnal Fizicheskoj Khimii 53:1171
40. Pil'nikov VP, Nikitin Yu S, Vladimirova NA, Kulatchek ES (1981) Zashtita Metallov (Prot Met) 17:135
41. Molenaar A (1981) US Pat 4 269 625
42. Molenaar A, Coumans JJC (1982) Surf Technol 16:265
43. Koyano H, Kato M, Uchida M (1991) Plat Surf Finish 78(7):68
44. Georgieva J, Kawashima S, Armyanov S, Valova E, Hubin A, Koyama Y, Steenhaut O, Haydu J, Delplancke J-L, Tsacheva Ts (2005) J Electrochem Soc 152:C783
45. Georgieva J, Armyanov S (2003) J Electrochem Soc 150:C760
46. Armyanov S, Vangelova T, Stoyanchev R (1982) Surf Technol 17:89
47. Armyanov S, Chakarova G, Vangelova T, Pozharlieva Ts (1986) Bulgarian Pat 47:282
48. Armyanov S, Sotirova G (1989) J Electrochem Soc 136:1575
49. Hung A (1988) Plat Surf Finish 75(1):62
50. Hung A (1988) Plat Surf Finish 75(1):74
51. Hung A, Chen KM (1989) J Electrochem Soc 136:72
52. Chassaing E, Cherkaoui M, Srhiri A (1993) J Appl Electrochem 23:1169
53. Hirth FW, Speckhardt H (1973) Galvanotechnik 64:452
54. Wiegand H, Hirth FW, Speckhardt H (1975) J Less-Common Met 43:267
55. Okamura Y, Futami S, Kawada K, Koga A, Matsui F (1987) J Met Finish Soc Japan 38:424
56. Lelental M (1975) J Electrochem Soc 122:486
57. Tachev D, Georgieva J, Armyanov S (2001) Electrochim Acta 47:359
58. Krolikowski A, Bielinski J, Jaworska A (2004) 4th KSCS, Mechanisms of Corrosion and Corrosion Prevention Proceedings, p.142, Editors: Olof Forsen, Jari Aromaa, Lea Selin, Helsinki University of Technology, Espoo, Finland